

VIDEOCAPILLAROSCOPIC MONITORING OF MICROCIRCULATION IN RATS DURING PHOTODYNAMIC THERAPY

Guryleva A.V.¹, Machikhin A.S.¹, Grishacheva T.G.², Petrishchev N.N.²

¹Scientific and Technological Center for Unique Instrumentation of the Russian Academy of Sciences, Moscow, Russia

²First St. Petersburg State Medical University named after Academician I.P. Pavlova, St. Petersburg, Russia

Abstract

The proposed approach to microcirculation assessment is non-invasive, informative, and can be implemented during photoactivation, and thus is perspective both for research tasks and clinical practice. The functional principles of the vasculature response to photodynamic exposure, identified using this technique, also foster the efficiency and safety of photodynamic therapy. The developed setup allows simultaneous photodynamic exposure and studying the microcirculation parameters by videocapillaroscopy and photoplethysmography techniques. Photodynamic action is carried out by 662 nm laser radiation with a power density of 15 mW/cm² in continuous and pulsed modes. The imaging system of the setup consists of a large working distance microscope, an optical filter, and a monochrome camera. The illumination system is based on LED with a central wavelength of 532 nm. The acquired images were processed in order to obtain morphometric and hemodynamic microcirculation data in the inspected skin area. To compare the proposed approach with existing methods, we measured blood flow parameters by a laser Doppler flowmeter. We tested the developed setup on rats injected with a photosensitizer and obtained active vessel maps, photoplethysmograms, and skin vessel density values before, during, and after photoactivation in both generation modes. The proposed approach allows to reveal differences in the microcirculation response to photodynamic effects of low power densities in different modes, in particular, the discrepancy between the time from the start of exposure to the cessation of blood flow and the start of the recovery period.

Key words: photodynamic therapy, microcirculation, photoplethysmography, videocapillaroscopy, laser Doppler flowmetry.

Contacts: Grishacheva T.G., e-mail: tgrishacheva@gmail.com

For citation: Guryleva A.V., Machikhin A.S., Grishacheva T.G., Petrishchev N.N. Videocapillaroscopic monitoring of microcirculation in rats during photodynamic therapy, *Biomedical Photonics*, 2023, vol. 12, no. 2, pp. 16–23. doi: 10.24931/2413–9432–2023–12-2-16–23.

ПРИМЕНЕНИЕ ВИДЕОКАПИЛЛЯРОСКОПИИ ДЛЯ МОНИТОРИНГА МИКРОЦИРКУЛЯЦИИ В КОЖЕ ПРИ ФОТОДИНАМИЧЕСКОЙ ТЕРАПИИ

А.В. Гурылева¹, А.С. Мачихин¹, Т.Г. Гришачева², Н.Н. Петрищев²

¹Научно-технологический центр уникального приборостроения Российской академии наук, Москва, Россия

²Первый Санкт-Петербургский государственный медицинский университет имени академика И.П. Павлова» Министерства здравоохранения Российской Федерации, Санкт-Петербург, Россия

Резюме

Предложено аппаратно-программное и методическое обеспечение для оценки микроциркуляции, которое отличается неинвазивностью, информативностью, а главное, возможностью проводить исследование в ходе фотоактивации, и может стать дополнением к существующим диагностическим методам как в исследовательских задачах, так и в клинической практике. Выявленные с помощью разработанного подхода функциональные принципы реакции сосудистой сети на фотодинамическое воздействие представляются полезными для повышения эффективности и безопасности фотодинамической терапии. Разработка и апробация методов видеокapилляроскопии и фотоплетизмографии для изучения ранних изменений микроциркуляции при фотодинамической активации. Разработанная установка позволяет одновременно проводить фотодинамическое воздействие и исследование параметров микроцир-

куляции методами видеокапилляроскопии и фотоплетизмографии. Фотодинамическое воздействие осуществляется через 3 ч после внутривенного введения фотосенсибилизатора на основе хлорина е6 (5 мг/кг) лазерным излучением с длиной волны 662 нм и плотностью мощности 15 мВт/см² в непрерывном и импульсном режимах. Визуализирующая система установки состоит из микроскопа с большим рабочим расстоянием, цифровой высокоскоростной камеры и оптического фильтра, отсекающего отраженное от исследуемой поверхности излучение фотоактивации. Осветительная система представлена диодным источником излучения с центральной длиной волны 532 нм. Зарегистрированные установкой изображения исследуемого участка кожи обрабатываются в разработанном авторами программном обеспечении для получения морфометрических и гемодинамических данных о микроциркуляции. Для сравнения предложенного подхода с существующими методами параметры кровотока регистрировали также лазерным доплеровским флоуметром. В ходе апробации разработанной установки на инъецированных фотосенсибилизатором крысах получены наборы карт действующих сосудов, фотоплетизмограмм и значений плотности сосудов кожи до, во время и после фотоактивации в двух режимах генерации. Проведен совместный анализ данных видеокапилляроскопии, фотоплетизмографии и лазерной доплеровской флоуметрии. Показано, что предложенный подход позволяет выявить различия в механизмах реакции микроциркуляции на фотодинамическое воздействие с малой плотностью мощности в различных режимах, в частности, несовпадение времени от начала экспозиции до остановки кровотока и начала восстановительного периода.

Ключевые слова: фотодинамическая терапия, микроциркуляция, фотоплетизмография, видеокапилляроскопия, лазерная доплеровская флоуметрия

Контакты: Гришачева Т.Г., e-mail: tgrishacheva@gmail.com

Ссылка для цитирования: Гурьева А.В., Мачихин А.С., Гришачева Т.Г., Петрищев Н.Н. Применение видеокапилляроскопии для мониторинга микроциркуляции в коже при фотодинамической терапии // Biomedical Photonics. – 2023. – Т. 12, № 2. – С. 16–23. doi: 10.24931/2413–9432–2023–12–2–16–23.

Introduction

Photodynamic therapy (PDT) is a treatment method based on a combination of a light-sensitive pharmacological drug, a photosensitizer (PS), and exposure to electromagnetic radiation of a certain wavelength. PS photoactivation initiates photochemical reactions, which are accompanied by the formation of reactive oxygen species (ROS), which have a cytotoxic effect on the cells of the treated tissues. PDT is used to treat a number of dermatological skin diseases, including acne, psoriasis, dermatosis, and some forms of skin cancer, such as basal cell and squamous cell carcinomas [1, 2]. The effect of PDT on microcirculation (MC) in the skin is of great importance for achieving a therapeutic effect.

The study of MC in the upper layers of the skin during photoactivation (PA) provides information on its functional response to PA, which is necessary to increase its effectiveness and safety of treatment, as well as to study the mechanisms of PDT action. Among the existing methods for studying MC in the skin to identify the features of the vascular response in tumor damage after PA, the most common method is laser Doppler flowmetry (LDF). It provides registration of changes in tissue perfusion integrally from a certain area of the skin based on the Doppler effect [3–5].

Laser spectroscopy is also used to analyze MC and study the mechanisms of photodynamic action. It is based on the use of spectral analysis of radiation reflected from the skin to determine in real time the content of oxygenated hemoglobin and deoxygenated hemoglobin in capillaries, which is one of the key indicators of the effectiveness of PDT [6]. There are known methods for assessing blood flow dynamics using fluorescent contrast agents,

including with the use of confocal microscopy [7, 8], which makes it possible to visualize *in vivo* the vascular network with high resolution and evaluate responses to PDT both at the level of vascular endothelial cells and at the level of a separate vessel. Optical coherence tomography makes it possible to visualize the capillary network and assess vascular occlusion after PDT both in the tumor and in surrounding healthy tissues [9].

Although most of the existing methods for diagnosing MC during PDT are non-invasive and can provide *in vivo* measurements, they do not allow monitoring directly during PA. In addition, the methods have a number of disadvantages, such as dependence on the orientation of the sensors and the experience of the operator, the need to use coloring agents, as well as the complexity and high cost of the equipment.

One of the promising methods for *in vivo* assessment of the morphological and functional characteristics of the capillary bed of the skin is video capillaroscopy (VCS) [10,11]. It is based on the registration of a sequence of skin images and their subsequent spatial-frequency analysis. The result of videocapillaroscopic studies is a map of active vessels with active blood flow, as well as hemodynamic characteristics, including a map of the speed of erythrocyte movement. VCS is featured in that it does not require the use of tinting agents, provides a spatial distribution of the studied parameters, is simple and accessible in technical implementation, and also provides comprehensive information on the morphometric and hemodynamic parameters of the microvasculature. In a number of studies, VCS is used to evaluate the PDT efficiency and determine the optimal photosensitizer doses and radiation parameters [12].

The equipment for VCS makes it possible to quantify tissue perfusion by recording and analyzing photoplethysmograms (PPGs). The amount of radiation reflected from the skin changes along with the optical density of the studied tissues, which in turn depends on the blood supply [13]. PPG is a temporal periodic signal proportional to the intensity of radiation reflected from the skin, which characterizes tissue perfusion and is used to assess MC in solving many biomedical problems [14–16].

An important property of the VCS methods and photoplethysmography is the non-contact measurements, which are important for monitoring during PA. However, to the best of our knowledge, no description of the implementation of such a study has been provided so far. In this paper, we consider the possibility of using VCS and photoplethysmography to study early changes in MC during PA, depending on the regime of laser radiation generation.

Materials and methods

Experimental animals

The study was conducted on the basis of the Pavlov First Saint Petersburg State Medical University of the Ministry of Health of Russia. The work was performed on male Wistar rats weighing 250 ± 25 g, obtained from the "Rappolovo" Laboratory Animals Nursery of the National Research Centre "Kurchatov Institute" in accordance with the EU directive (The European Council Directive (86/609 /EEC)) on the observance of ethical principles in work with laboratory animals. The animals were kept on unlimited intake of food (standard diet for laboratory rats K-120 (Informkorm, Russia)) and water at a standard twelve-hour regimen (12 h in light, 12 h in dark). The temperature was maintained within 22–25°C, and the relative humidity was 50–70%. The duration of the quarantine (acclimatization period) for all animals was at least 14 days.

Before the start of the experiment, the animals were anesthetized by intravenous administration of Zoletil 100 (VIRBAC, France) and Xyla (De Adelaar B.V., Netherlands) in equal volumes at a dose of 0.5 ml/kg. Then the rat was

placed on a thermostated table TCAT-2 (Physitemp, USA) with constant maintenance of rectal temperature within 37–37.5°C. The skin of the back was cleaned of coat mechanically. The rats were divided into 2 groups. For the first group, PA was performed in a continuous generation mode, and for the second, in a pulsed generation mode. Intact rats were used as controls. The study of MC in the skin was carried out 3 hours after the administration of a photosensitizer based on chlorin e6, radachlorin (RADA-PHARMA, Russia), at a dose of 5 mg/kg into the tail vein.

Equipment

To assess the MC during PDT, a setup containing a PDT laser source and a video conferencing system has been developed and tested (Fig. 1). The VCS system includes a LED source with a center wavelength of 520 nm and a bandwidth of 30 nm (LED), a microscope (M) with a long working distance and x1.5 magnification, a monochrome camera (C) (Allied Vision Procolica GT2000, Germany) with a resolution of 2048×1088 pixels, a pixel size of $5.5 \times 5.5 \mu\text{m}$, a frame rate of up to 54 Hz, a GigE interface, and a 12-bit ADC and a computer (PC). The selected irradiation wavelength allows for increasing the contrast of capillaries against the background of surrounding tissues. The microscope and camera provide high resolution, magnification, and frame-rate imaging of the rat skin. To provide a sharp image throughout the entire field of view, the region under study was covered with a thin glass plate (GP). To obtain images under the same conditions before, during, and after PDT, an optical filter (F) was placed in front of the microscope to cut off radiation in the spectral range above 570 nm. An optical fiber (OF) with a microlens that transmits PA laser radiation from an ALOD laser device (L) (Alkom Medica, Russia) with a wavelength of 662 nm and a power density of 15 mW/cm^2 was fixed in a position that provides the diameter of the laser spot of 3 cm on the tissue under study.

Blood flow was measured using both the VSC and LDF (Transonic Systems Inc., BLF21). The power of the LDF diode radiation source with a wavelength of 780 nm

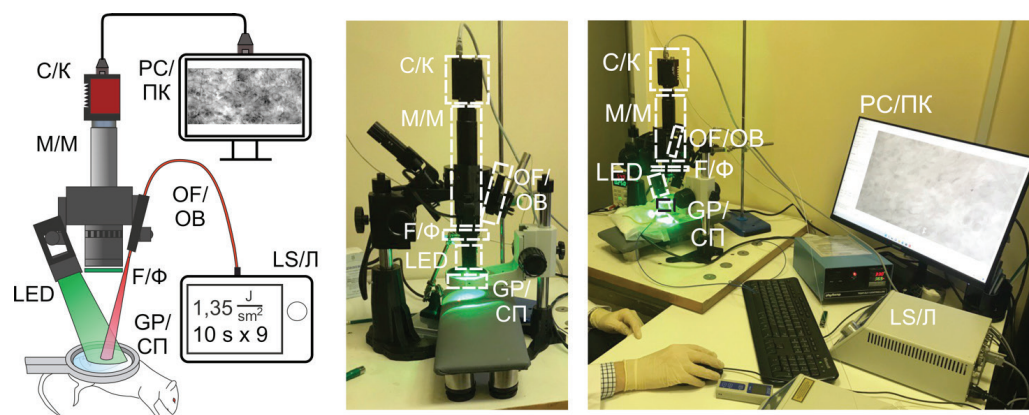


Рис. 1. Схема установки (К – камера, М – микроскоп, ПК – персональный компьютер, ОБ – оптическое волокно, Л – лазерный аппарат, Ф – оптический фильтр, СП – стеклянная пластина).
Fig. 1. Assembled setup (C – Camera, M – Microscope, PC – personal computer, OF – optical fiber, LS – laser, F – optical filter, GP – glass plate).

did not exceed 2 mW. The flowmeter allowed to register tissue perfusion from 0 to 100 ml/min per 100 g of tissue. The results were evaluated in perfusion units (pf. un.). The volume of the zone studied with the help of a laser sensor did not exceed 1 mm³, and the depth of probing microhemodynamics was up to 1 mm.

Experiment Protocol

The scheme of the experiment is shown in Fig. 2. The MC parameters were estimated for two PA modes. The exposure in the continuous mode was 1.5 min, the exposure in the pulsed mode was 3 min, while the pulse duration and the interval between pulses were 10 s. The energy density in both groups was 1.35 J/cm².

Video capillaroscopic examination was performed 1.5 min before, during, and 20 min after PA. Before and after PA, image sequences of 1000 12-bit frames were recorded at a frame rate of 43 Hz. For a detailed analysis of changes in the MC during the exposure, shooting was

carried out at the same frame rate, but for a time equal to the duration of the PDT time pulse, i.e., 10 s.

The fixation of blood flow parameters during PA using LDF was not performed due to the contact nature of the method; therefore, the data were recorded before and after PA. To reduce the effect of interference, the information was read three times for 1 min and the smallest value was recorded. The MC index (IM) was recorded before PA for 1 min and immediately after turning off the laser radiation for 20 min. To exclude the effect of LDF radiation on MC in the skin of PS-introduced rats, the measurements on intact rats have been performed without PS as an IM control.

Digital data processing algorithm for VCS

The image sequences obtained by the VCS method were processed using the algorithm implemented in MATLAB and described in detail in [17]. The main stages of the algorithm are shown in Fig. 3. The pre-processing

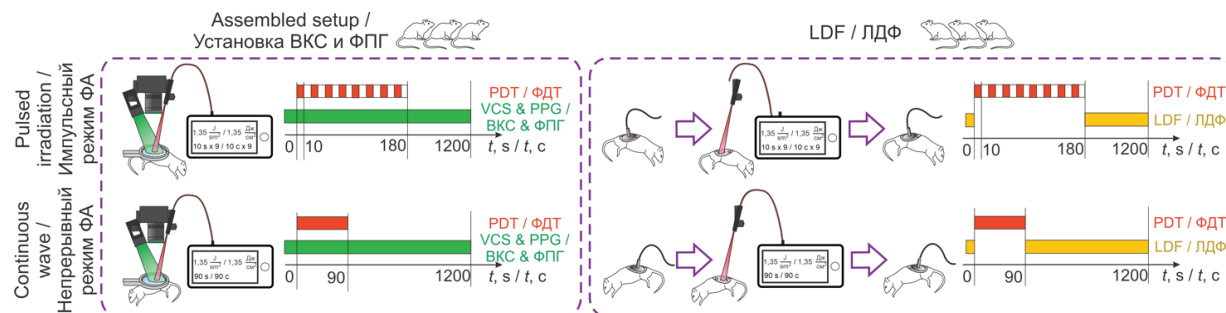


Рис. 2. Протокол эксперимента (ВКС – видеокапилляроскопия, ФПГ – фотоплетизмография, ЛДФ – лазерная Допплеровская флоуметрия, ФДТ – фотодинамическая терапия, ФА – фотоактивация).

Fig. 2. Experimental design (VCS – videocapillaroscopy, PPG – photoplethysmography, PDT – photodynamic therapy, LDF – laser Doppler flowmetry).

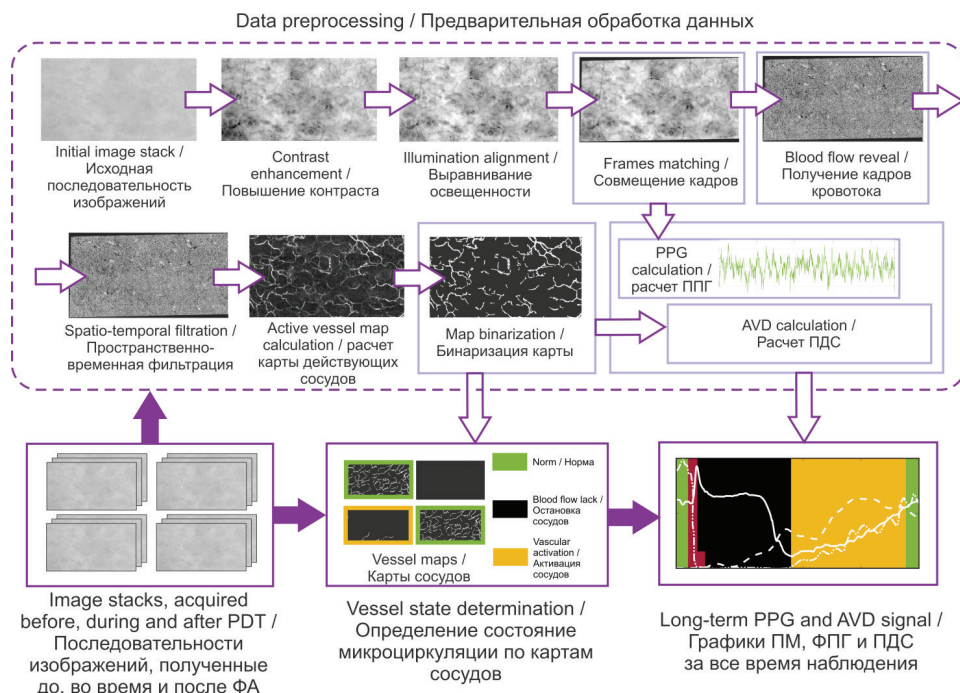


Рис. 3. Алгоритм цифровой обработки данных видеокapилляроскопии и фотоплетизмограмм (ППГ – фотоплетизмография, ПДС – плотность действующих сосудов, ПМ – показатель микроциркуляции, ФА – фотоактивация).

Fig. 3. Data processing pipeline (PPG – photoplethysmography, AVD – active vessel density, PDT – photodynamic therapy).

data is used to improve images, in particular, to expand the dynamic range, eliminate illumination nonuniformity, compensate for sample displacement, etc.

Enhanced images consist of pixels related to vessels and their surrounding tissues. Within each sequence in the pixels related to the vessels, there is a periodic change in intensity associated with the movement of red blood cells. The intensities of the pixels of the tissues surrounding the vessels have practically unchanged values. With the help of spatial frequency analysis, vessel maps were calculated for each image sequence. For each such map, the density of active vessels measured as a percentage can be calculated as the ratio of pixels belonging to the active capillary network to the total number of image pixels. The time points associated with the onset of vascular shutdown, complete stopping of blood flow, and vascular activation were determined using a visual analysis of the resulting map, based on which the graph was further marked.

A decrease or increase in the optical density of the studied area, modulated by heart rate and blood supply, leads to a corresponding change in the intensity of image pixels from frame to frame. Averaging the pixel intensity of each image of all registered sequences makes it possible to obtain a set of points equal to the number of frames. Such points form a PPG that describes perfusion during the experiment and is measured in relative units (rel. un.). Further, the low-frequency component is removed from the PPG signal and only the amplitude of local periodic changes in the signal associated with the heart rhythm is analyzed. However, in the present work, for long-term perfusion analysis, the low-frequency component is also a useful signal. The PPG signal was subjected only to smoothing by the sliding window method to eliminate the noise component.

Results

Data on the state of MC in the skin during PDT using the developed VCS and LDF setups are shown in Fig. 4. Maps of vessels, PPG, curves of changes in vascular density, blood flow velocity, and MC (IM) are shown on one graph for two PA modes. The graphs are marked with colors following the state of the vessels based on the analysis of maps and vessel density.

According to LDF data, the IM in the skin before exposure ranged from 2.3 to 6.5 pf. un., and the average value was 4.7 ± 0.5 pf. un. Immediately after PA in the continuous mode of laser generation, a decrease in the IM to 0.4 ± 0.4 pf. un. was observed. During the first 7 minutes there was a gradual increase in IM and by 8 minutes this indicator was 3.7 ± 0.3 pf. un. During the subsequent registration of blood flow for 10 min, there was a significant increase in the IM in the skin up to 9.9 ± 0.7 pf. un. On the 20th min of registration, the IM was 7.2 ± 0.4 pf. un.

In the group of rats that were exposed to the pulse mode, immediately after PA, a decrease in IM to 0.6 ± 0.4 pf. un. was registered. By 4 min of observation of MCR in the skin, the IM was 4.7 ± 0.3 pf. un. Then there was an increase in IM to 14.5 ± 0.8 pf. un. By the end of the time of monitoring the blood flow, the IM was 7.4 ± 0.4 pf. un.

Before PA, the initial values of PPG and AVD were, respectively, from 0.4 to 0.8 rel. un. and from 7.1% to 11.9%. During laser exposure, a decrease in AVD and an increase in PPG amplitude were observed. The decrease in AVD in the group with continuous PA occurred on average by 39 s of laser exposure, which corresponds to 0.585 J/cm^2 . In the group with the pulsed generation, a decrease in the same values was recorded on average by 44 s, that is, when the energy density reached 0.33 J/cm^2 . At the same time, the complete absence of blood flow in the group of continuous irradiation was recorded on average for 96 s, that is, 6 s after the termination of laser exposure. In the pulse mode group, the complete absence of blood flow was registered at 128 s, which means during PA.

The recovery period, accompanied by the appearance of blood flow, in the group with a continuous mode of exposure began on average 8 minutes after the start of laser exposure, which coincided with the moment when the PPG values began to increase. Registration of restoration of blood flow in the pulsed mode occurred 4.7 minutes after the end of laser exposure, however, an increase in PPG values occurred later, on average, after 7.5 minutes.

Discussion

PDT has established itself as an effective method for the treatment of malignant neoplasms and a number of non-tumor diseases [18,19]. During PA, the energy of laser radiation is absorbed and transferred to the conjugated system of the PS molecule. The interaction of a photoactivated PS molecule with an oxygen molecule leads to the transfer of electronic excitation energy to the molecular oxygen of the medium, followed by its transfer to a more reactive state and the formation of ROS, causing lipid and protein peroxidation in cell membranes, causing their damage and death. In addition, in the mechanism of biological action in PDT, the violation of the MCR, as well as the local response to immune reactions, is important. The state of the MCR provides a certain content of oxygen necessary for the formation of its active forms in the PA zone, as well as the delivery of immune-competent cells.

One of the parameters influencing the result of photodynamic action is the mode of radiation generation. In practice, as a rule, a continuous mode of radiation generation is used, which consists in irradiating a skin area during the entire exposure time with

radiation with constant characteristics and leading to intense depletion of ROS as a result of photochemical reactions [20, 21]. The pulse mode, which is characterized by successive periods of turning the laser source on and off during exposure, makes it possible to reduce this effect [23, 24]. Evaluation of the influence of different regimens on MC remains relevant, allowing to increase the effectiveness of therapy. In the work, a multiparametric analysis of MC blood flow was carried out by various methods.

The reflectivity of the skin is largely determined by the filling of tissue with blood and its oxygenation. With an increase in blood supply and oxygenation, there is an increase in absorption and a decrease in the reflectivity of the tissue. An increase in PPG corresponds to a greater amount of radiation incident on the sensor of the video camera and hence reflected from the surface under study. A rise in the PPG value in the first minutes of PA (Fig. 4, red zone) may indicate a decrease in the amount of blood in the measured area of the skin, together with the degree of its oxygenation. The dose of laser PA was insignificant, therefore, for some time after the end of PA, the mechanism of autoregulation was triggered. The decrease in the value of PPG during the period of complete cessation of blood flow (Fig. 4, black zone) is due to the activation of regulatory mechanisms and changes in MC in the deeper layers of the skin, causing a rush of oxygenated blood to the site of

exposure. An increase in the IM values recorded by LDF corresponds to the same processes. The result of regulatory processes after the termination of PA is the restoration of blood flow in the vessels accessible for visualization by VCS (Fig. 4, yellow zone) and the subsequent return to an equilibrium state with an increase in PPG and a decrease in IM to values close to the initial ones (Fig. 4, green zone).

In both continuous and pulsed modes, PA led to a stop in the movement of erythrocytes through the vessels, as well as to a change in the values of PPG, IM, and AVD, which returned to their original or close values 15 min after the beginning of PA. However, the nature of the response of rat skin microvessels to low doses of PA turned out to be different for the two regimens. In the group of animals subjected to PA in the pulsed mode, the beginning of the recovery period (Fig. 4, yellow zone), i.e., the return to the initial values of PPG, IM, and AVD, was observed earlier than in the group with continuous PA. Moreover, in the recovery period for the pulsed PA group, a local increase in IM by more than 3 times relative to the norm was observed, followed by a decrease to normal values.

The data obtained, showing the return of PPG and AVD to the initial values in the recovery period, correlate with the corresponding increase in IM obtained using LDF. At the same time, during the period of complete stoppage of blood flow in the superficial vessels

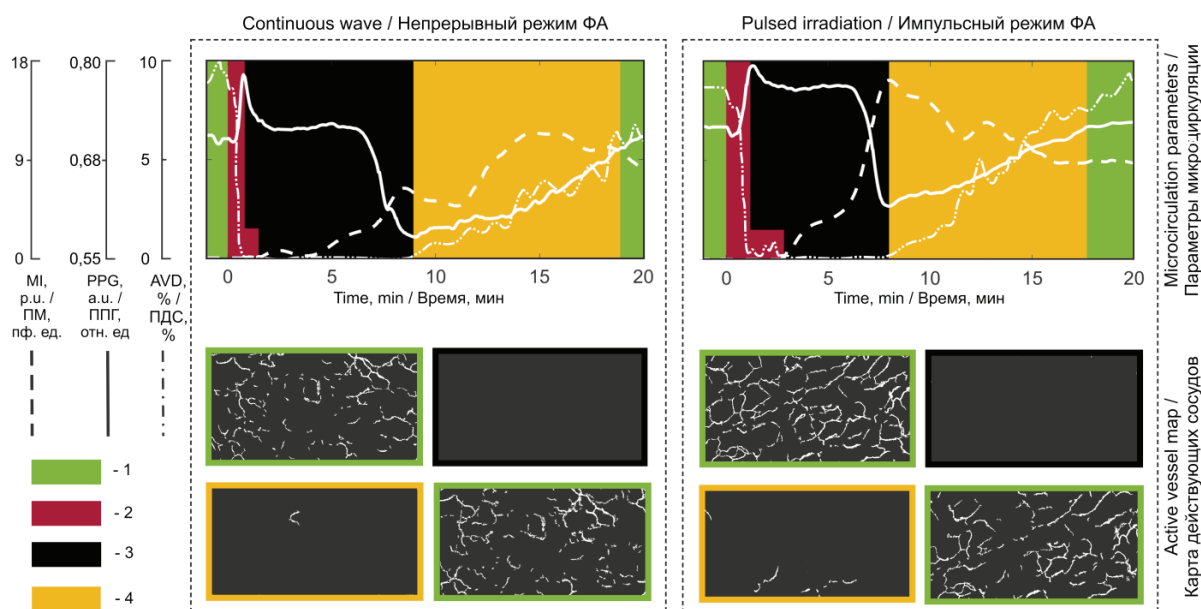


Рис. 4. Морфометрические и гемодинамические параметры микроциркуляции, полученные методами видеокапилляроскопии, фотоплетизмографии и лазерной доплеровской флоуметрии, для периодов соответствующих: 1 – нормальному состоянию сосудов относительно значений ФПГ, 2 – фотоактивации, 3 – остановке кровотока, 4 – восстановительному периоду (ПМ – показатель микроциркуляции, ППГ – фотоплетизмография, ПДС – плотность действующих сосудов, ФА – фотоактивация).

Fig. 4. Morphometric and hemodynamic microcirculation parameters acquired by means of videocapillaroscopy, photoplethysmography, and laser Doppler flowmetry: 1 – normal vessel functioning, 2 – photodynamic activation, 3 – cessation of blood flow, 4 – vascular activation (MI – microcirculation index, PPG – photoplethysmography, AVD – active vessel density).

and zero values of the AVD, the IM had non-zero values. Such differences may indicate the registration of MC parameters from different depths relative to the skin surface by different methods. Thus, with the help of LDF, blood flow parameters in the skin are examined at a depth of up to 1 mm, that is, in the capillaries and superficial arteriovenular plexus [20]. At the same time, VCS provides visualization of vessels lying at a depth of up to 0.5–1 mm [25, 26].

Conclusion

The results of this study showed the fundamental possibility of using the developed setup and method for monitoring skin MC during PDT, including directly during PA. The data obtained correlate with modern ideas about the mechanisms of the reaction of MC to PA and with the results obtained by methods common in practice [27, 28].

A methodical approach and its hardware-software implementation have been developed and tested, providing non-invasive obtaining of vascular maps, PPG, and AVD graphs before, after, and most importantly, during PA. A study of the mechanisms of skin reaction in different modes of generating photodynamic exposure at low doses of PA was performed using the proposed approach. For two modes of generation, the difference in time intervals between the beginning of PA, the stoppage of blood flow in the vessels, and the beginning of the recovery period, as well as in the duration of the latter, is shown. The described method of multiparametric assessment of the vasculature can serve as a valuable addition to the existing methods for the analysis of MC in research tasks and clinical practice.

The study was carried out within the State Assignment of the STC UI RAS (project FFNS-2022-0010).

REFERENCES

1. Dougherty T.J. et al. Photodynamic Therapy JNCI: Journal of the National Cancer Institute. *Oxford Academic*, 1998. Vol. 90(12), pp. 889-905.
2. Li X. et al. Clinical development and potential of photothermal and photodynamic therapies for cancer. *Nature Publishing Group*, 2020, Vol. 17(11), pp. 657-674.
3. Korbely M. et al. Nitric oxide production by tumour tissue: impact on the response to photodynamic therapy. *Br J Cancer. Nature Publishing Group*, 2000, Vol. 82(11), p. 1835.
4. Souza C.S. et al. Long-term follow-up of topical 5-aminolaevulinic acid photodynamic therapy diode laser single session for non-melanoma skin cancer. *Photodiagnosis Photodyn Ther*, 2009, Vol. 6 (3-4), pp. 207-213.
5. Chen D. et al. Intraoperative monitoring of blood perfusion in port wine stains by laser Doppler imaging during vascular targeted photodynamic therapy: A preliminary study. *Photodiagnosis Photodyn Ther. Elsevier*, 2016, Vol. 14, pp. 142-151.
6. Orlova A. et al. Diffuse Optical Spectroscopy Monitoring of Experimental Tumor Oxygenation after Red and Blue Light Photodynamic Therapy. *Photonics 2022*, Vol. 9, p. 19. *Multidisciplinary Digital Publishing Institute*, 2021. Vol. 9(1), p. 19.
7. Khurana M. et al. Intravital high-resolution optical imaging of individual vessel response to photodynamic treatment. *J Biomed Opt*, 2008, Vol. 13(4), p. 1.
8. Grishacheva T.G. et al. Digital Analysis of Colposcopic Images Before and After Photodynamic Therapy with Open Source Software ImageJ and Fluorescence diagnostics. *Optica Publishing Group*, 2020, p. JW3A.2.
9. Christou E.E. et al. Evaluation of the choriocapillaris after photodynamic therapy for chronic central serous chorioretinopathy. A review of optical coherence tomography angiography (OCT-A) studies. *Graefes Arch Clin Exp Ophthalmol. Graefes Arch Clin Exp Ophthalmol*, 2022, Vol. 260(6), pp. 1823-1835.
10. Gallucci F. et al. Indications and results of videocapillaroscopy in clinical practice. *Advances in medical sciences*, 2008, Vol. 53(2), pp. 149-157.
11. Machikhin A.S. et al. Exoscope-based videocapillaroscopy system for in vivo skin microcirculation imaging of various body areas. *Biomedical Optics Express*, 2021, Vol. 12(8), pp. 4627-4636. *Optica Publishing Group*, 2021, Vol. 12(8), pp. 4627-4636.
12. Da Silva F.A.M., Newman E.L. Dynamic capillaroscopy: a minimally invasive technique for assessing photodynamic effects in vivo. *Photochem Photobiol. John Wiley & Sons, Ltd*, 1993, Vol. 58(6), pp. 884-889.

ЛИТЕРАТУРА

1. Dougherty T.J. et al. Photodynamic Therapy JNCI: Journal of the National Cancer Institute // *Oxford Academic*. – 1998. – Vol. 90(12). – P. 889-905.
2. Li X. et al. Clinical development and potential of photothermal and photodynamic therapies for cancer // *Nature Publishing Group*. – 2020. – Vol. 17(11). – P. 657-674.
3. Korbely M. et al. Nitric oxide production by tumour tissue: impact on the response to photodynamic therapy // *Br J Cancer. Nature Publishing Group*. – 2000. – Vol. 82(11). – P. 1835.
4. Souza C.S. et al. Long-term follow-up of topical 5-aminolaevulinic acid photodynamic therapy diode laser single session for non-melanoma skin cancer // *Photodiagnosis Photodyn Ther*. – 2009. – Vol. 6 (3-4). – P. 207-213.
5. Chen D. et al. Intraoperative monitoring of blood perfusion in port wine stains by laser Doppler imaging during vascular targeted photodynamic therapy: A preliminary study // *Photodiagnosis Photodyn Ther. Elsevier*. – 2016. – Vol. 14. – P.142-151.
6. Orlova A. et al. Diffuse Optical Spectroscopy Monitoring of Experimental Tumor Oxygenation after Red and Blue Light Photodynamic Therapy // *Multidisciplinary Digital Publishing Institute*. – 2021. – Vol. 9(1). – P. 19.
7. Khurana M. et al. Intravital high-resolution optical imaging of individual vessel response to photodynamic treatment // *J Biomed Opt. J Biomed Opt*. – 2008. – Vol. 13(4). – P. 1.
8. Grishacheva T.G. et al. Digital Analysis of Colposcopic Images Before and After Photodynamic Therapy with Open Source Software ImageJ and Fluorescence diagnostics // *Optica Publishing Group*. – 2020. – P. JW3A.2.
9. Christou E.E. et al. Evaluation of the choriocapillaris after photodynamic therapy for chronic central serous chorioretinopathy. A review of optical coherence tomography angiography (OCT-A) studies // *Graefes Arch Clin Exp Ophthalmol. Graefes Arch Clin Exp Ophthalmol*. – 2022. – Vol. 260(6). – P. 1823-1835.
10. Gallucci F. et al. Indications and results of videocapillaroscopy in clinical practice // *Advances in medical sciences*. – 2008. – Vol. 53(2). – P. 149-157.
11. Machikhin A.S. et al. Exoscope-based videocapillaroscopy system for in vivo skin microcirculation imaging of various body areas. *Optica Publishing Group*. – 2021. – Vol. 12(8). – P. 4627-4636.
12. Da Silva F.A.M., Newman E.L. Dynamic capillaroscopy: a minimally invasive technique for assessing photodynamic effects in vivo // *Photochem Photobiol. John Wiley & Sons, Ltd*. – 1993. – P. Vol. 58(6). – P. 884-889.

13. Kamshilin A.A. et al. A new look at the essence of the imaging photoplethysmography. *Scientific Reports. Nature Publishing Group*, 2015. Vol. 5(1), pp. 1-9.
14. Kumar M. et al. PulseCam: a camera-based, motion-robust and highly sensitive blood perfusion imaging modality. *Scientific Reports*, 2020, Vol. 10(1), Nature Publishing Group, 2020. Vol. 10(1), pp. 1-17.
15. Park J. et al. Photoplethysmogram Analysis and Applications: An Integrative Review. *Front Physiol. Frontiers Media S.A.*, 2022, Vol. 12, p. 2511.
16. Allen J. Photoplethysmography and its application in clinical physiological measurement. *Physiol Meas*, 2007. Vol. 28(3).
17. Guryleva A.V. et al. Feasibility of videocapillaroscopy for characterization of microvascular patterns in skin lesions. *Proceedings of SPIE – The International Society for Optical Engineering*, 2022, Vol. 12147.
18. Dolmans D.E.J.G.J., Fukumura D., Jain R.K. Photodynamic therapy for cancer. *Nature Reviews Cancer*, 2003, Vol. 3(5). *Nature Publishing Group*, 2003, Vol. 3(5), pp. 380-387.
19. Gunaydin G., Gedik M.E., Ayan S. Photodynamic Therapy—Current Limitations and Novel Approaches. *Front Chem. Frontiers Media S.A.*, 2021. Vol. 9. P. 400.
20. Foster T., et al. Oxygen consumption and diffusion effects in photodynamic therapy. *Radiat. Res*, 1991, Vol. 126, pp. 296-303.
21. Henderson B., et al. Oseroff, Photofrin photodynamic therapy can significantly deplete or preserve oxygenation in human basal cell carcinomas during treatment, depending on fluence rate. *Cancer Res*, 2000, Vol. 60, pp. 525-529.
22. Klimenko V.V., et al. Pulse mode of laser photodynamic treatment induced cell apoptosis. *Photodiagnosis Photodyn Ther*, 2016, Vol. 13, pp. 101-107.
23. Wilson B.C., Patterson M.S. The physics, biophysics and technology of photodynamic therapy. *Phys Med Biol*, 2008, Vol. 53(9), pp. 61-109.
24. Abbot N.C. et al. Laser Doppler Perfusion Imaging of Skin Blood Flow Using Red and Near-Infrared Sources. *Journal of Investigative Dermatology Elsevier*, 1996, Vol. 107(6), pp. 882-886.
25. Moço A., Verkruysse W. Pulse oximetry based on photoplethysmography imaging with red and green light: Calibratability and challenges. *J Clin Monit Comput. Springer Science and Business Media B.V.*, 2021, Vol. 35(1), pp. 123-133.
26. Han S. et al. Design of Multi-Wavelength Optical Sensor Module for Depth-Dependent Photoplethysmography. *Multidisciplinary Digital Publishing Institute*, 2019. Vol. 19(24), p. 5441.
27. Volkov M. V et al. Evaluation of blood microcirculation parameters by combined use of laser. *Doppler flowmetry and videocapillaroscopy methods*, 2017.
28. Dremmin V. et al. Dynamic evaluation of blood flow microcirculation by combined use of the laser Doppler flowmetry and high-speed videocapillaroscopy methods. *J Biophotonics*, 2019, Vol. 12(6).
13. Kamshilin A.A. et al. A new look at the essence of the imaging photoplethysmography. *Scientific Reports. Nature Publishing Group*. – 2015. – Vol. 5(1). – P. 1-9.
14. Kumar M. et al. PulseCam: a camera-based, motion-robust and highly sensitive blood perfusion imaging modality // *Nature Publishing Group*. – 2020. – Vol. 10(1). – P. 1-17.
15. Park J. et al. Photoplethysmogram Analysis and Applications: An Integrative Review // *Front Physiol. Frontiers Media S.A.* – 2022. – Vol. 12. – P. 2511.
16. Allen J. Photoplethysmography and its application in clinical physiological measurement // *Physiol Meas. Physiol Meas.* – 2007. – Vol. 28(3). – C. R1
17. Guryleva A.V. et al. Feasibility of videocapillaroscopy for characterization of microvascular patterns in skin lesions // *Proceedings of SPIE – The International Society for Optical Engineering*. – 2022. – Vol. 12147.
18. Dolmans D.E.J.G.J., Fukumura D., Jain R.K. Photodynamic therapy for cancer // *Nature Publishing Group*. – 2003. – Vol. 3(5). – P. 380-387.
19. Gunaydin G., Gedik M.E., Ayan S. Photodynamic Therapy—Current Limitations and Novel Approaches // *Front Chem. Frontiers Media S.A.* – 2021. – Vol. 9. – P. 400.
20. Foster T., et al. Oxygen consumption and diffusion effects in photodynamic therapy // *Radiat. Res.* – 1991. – Vol. 126. – P. 296-303.
21. Henderson B., et al. Oseroff, Photofrin photodynamic therapy can significantly deplete or preserve oxygenation in human basal cell carcinomas during treatment, depending on fluence rate // *Cancer Res.* – 2000. – Vol. 60. – P. 525-529.
22. Klimenko V.V., et al. Pulse mode of laser photodynamic treatment induced cell apoptosis // *Photodiagnosis Photodyn Ther.* – 2016. – Vol. 13. – P. 101-107.
23. Wilson B.C., Patterson M.S. The physics, biophysics and technology of photodynamic therapy // *Phys Med Biol.* – 2008. – Vol. 53(9). – P. 61-109.
24. Abbot N.C. et al. Laser Doppler Perfusion Imaging of Skin Blood Flow Using Red and Near-Infrared Sources // *Journal of Investigative Dermatology Elsevier*. – 1996. – Vol. 107(6). – P. 882-886.
25. Moço A., Verkruysse W. Pulse oximetry based on photoplethysmography imaging with red and green light: Calibratability and challenges. *J Clin Monit Comput // Springer Science and Business Media B.V.* – 2021. – Vol. 35(1). – P. 123-133.
26. Han S. et al. Design of Multi-Wavelength Optical Sensor Module for Depth-Dependent Photoplethysmography // *Multidisciplinary Digital Publishing Institute*. – 2019. – Vol. 19(24). – P. 5441.
27. Volkov M. V et al. Evaluation of blood microcirculation parameters by combined use of laser // *Doppler flowmetry and videocapillaroscopy methods*. – 2017.
28. Dremmin V. et al. Dynamic evaluation of blood flow microcirculation by combined use of the laser Doppler flowmetry and high-speed videocapillaroscopy methods // *Journal of biophotonics*. – 2019. – T. 12. – №. 6. – C. e201800317.